UNIVERSITY OF WEST BOHEMIA

Applied and Computational Mechanics 3 (2009) 287–296

Applied and Computational Mechanics

Analysis of composite car bumper reinforcement

V. Kleisner[a,*], R. Zemčík[a]

[a] *Faculty of Applied Sciences, University of West Bohemia, Univerzitní 22, 306 14 Plzeň, Czech Republic*

Received 30 August 2008; received in revised form 3 November 2009

Abstract

The presented work summarizes the present state of car passive safety testing according to European methodologies. The main objective is to analysis a bumper reinforcement made of composite materials. The bumper is tested according to RCAR (Research Council for Automobile Repairs) methodology using numerical simulation. Individual proposed variants are compared with the existing steel construction which does not comply with manufacturers specifications. The PAM-Crash software is used for the simulation. The numerical model is using shell elements and the Ladevèze model for the description of behaviour of composite materials. The methodology for the set-up of the numerical model in PAM-crash is firstly validated by comparison of experiment and analytical results.

Keywords: passive safety, finite element method, RCAR, composite materials, bumper reinforcement

1. Introduction

Car accidents are happening every day. Most drivers are convinced that they can avoid such troublesome situations. Nevertheless, we must take into account the statistics – ten thousand dead and hundreds of thousands to million wounded each year. These numbers call for the necessity to improve the safety of automobiles during accidents. As a result most present-day automobiles have at least safety belts with retractors and airbags [6]. However, car accident does not necessarily mean bodily harm. In a low-speed car accident only physical damage occurs, assuming that basic safety regulations, such as fastened seat belts, are kept.

This work focuses on the application of composite materials in a frontal bumper system. In recent years, composite materials have been more frequently used in industry and they have progressively replaced metal materials. This trend is caused by their high strength (and stiffness) to mass ratio and the ability to produce parts with required mechanical properties. The main objective is to analysis the bumper reinforcement made of composite materials and to compare it with the original steel bumper reinforcement in terms of its stiffness and damage behaviour, and mass reduction.

2. European car testing

2.1. EuroNCAP

EuroNCAP [5] company was founded in 1997 and has two main objectives. Firstly, it provides information about comparable automobile safety rating. Secondly, it tries to motivate producers to improve automobile safety and thereby reduces the number of wounded passengers. This

*Corresponding author. Tel.: +420 377 632 336, e-mail: kleisner@kme.zcu.cz.

task is progressively fulfilled in conjunction with automobile producers. The testing stems from EEVC (European Enhanced Vehicle-safety Committee) procedures.

The tests implemented by EuroNCAP are:

- frontal impact,
- side impact,
- pole impact,
- child protection,
- pedestrian protection.

2.2. *RCAR*

RCAR [4], the Research Council for Automobile Repairs, is an international organization that works towards reducing insurance costs by improving automotive damage ability, repair ability, safety and security by low-speed offset car crash test.

The test vehicle speed shall be 15 km/h within a one-meter distance from the barrier. The barrier offset of the test vehicle is 40 %. The barrier is skewed in a 10 degrees angle and has a radius of 150 mm as shown in Fig. 1.

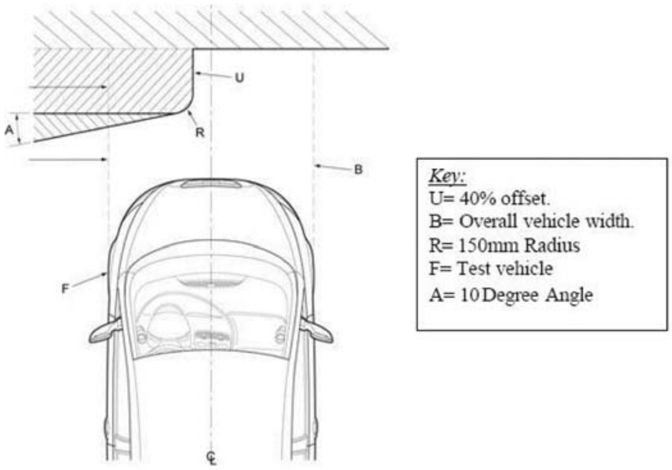

Fig. 1. Scheme of RCAR test

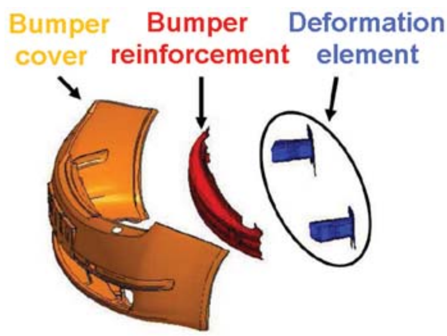

Fig. 2. Frontal bumper system components

3. Bumpers

Bumpers are fixed on the front and on the back side of a car and serve as its protection. They reduce the effects of collision with other cars and objects due to their large deformation zones. The bumpers are designed and shaped in order to deform itself and absorb the force (kinetic energy) during a collision. The whole frontal bumper system consists the following parts (also seen in Fig. 2):

- the cover,
- the mechanical and deformation energy absorber,
- the bumper reinforcement.

4. Composite damage model in PAM-Crash

The Ladevèze model [3] is dedicated to the numerical simulation of unidirectional continuous fiber reinforced composite materials. Unlike the heterogeneous "biphase" model, the Ladevèze model does not treat the two phases separately (fibers and matrix). Instead the composite ply is described by homogeneous continuum mechanics. In this model some damages related to experimentally observed phenomena are included (see Fig. 3).

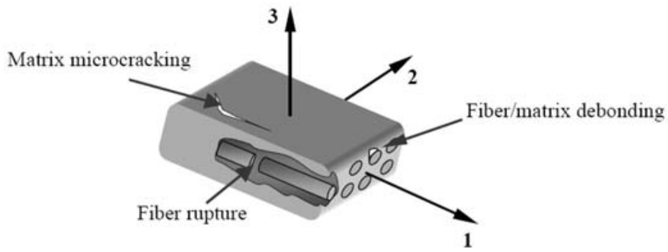

Fig. 3. Composite ply damages

The constitutive relationship of the Ladevèze model can be expressed as follows [3]:

$$\begin{bmatrix} \varepsilon_{11}^e \\ \varepsilon_{22}^e \\ 2\varepsilon_{12}^e \\ 2\varepsilon_{23}^e \\ 2\varepsilon_{13}^e \end{bmatrix} = \begin{bmatrix} 1/E_1 & -\nu_{12}^0/E_1 & 0 & 0 & 0 \\ -\nu_{12}^0/E_1 & 1/E_2 & 0 & 0 & 0 \\ 0 & 0 & 1/G_{12} & 0 & 0 \\ 0 & 0 & 0 & 1/G_{23} & 0 \\ 0 & 0 & 0 & 0 & 1/G_{12} \end{bmatrix} \begin{bmatrix} \sigma_{11} \\ \sigma_{22} \\ \sigma_{12} \\ \sigma_{23} \\ \sigma_{13} \end{bmatrix}, \tag{1}$$

where

1. fiber direction: $E_1 = E_1^0(1 - d^{ft})$
2. transverse direction: $E_2 = E_2^0(1 - d')$
3. for shear: $G_{12} = G_{12}^0(1 - d)$

In these equations d^{ft} is the fiber damage constant and d' and d are the matrix damage constants.

Elastic matrix damaging behavior

The matrix related damages are taken into account by two scalar variables, d and d'. These variables express an experimentally displayed phenomena: parameter d quantifies the damage which comes from the debonding between fibers and matrix, whereas parameter d' is related to the damage due to the microcracking of the matrix parallel to the fiber direction.

The damage functions, Z_d and Z_d', associated respectively with d and d' are defined by the expressions

$$\frac{\partial E_D}{\partial d} = Z_d = \frac{1}{2}\frac{\sigma_{12}^2 + \sigma_{13}^2}{G_{12}^0(1-d)^2}, \tag{2}$$

$$\frac{\partial E_D}{\partial d'} = Z_d' = \frac{1}{2}\frac{\langle\sigma_{22}\rangle_+^2}{E_2^0(1-d')^2}, \tag{3}$$

where (2) is shear damage and (3) is transverse damage. E_D is elastic strain energy and $\langle a\rangle_+ = a$, if $a > 0$, else $a = 0$.

The damage evolution functions over time t are defined as

$$Y(t) = \sup_{\tau \geq t} \sqrt{Z_d(\tau) + bZ'_d(\tau)} \tag{4}$$

$$Y'(t) = \sup_{\tau \geq t} \sqrt{Z'_d(\tau)}. \tag{5}$$

The damage values d and d' are calculated from

$$d = \frac{\langle Y(t) - Y_0 \rangle_+}{Y_c}, \quad \text{if } d < d_{\max},\ Y'(t) < Y'_S \text{ and } Y(t) < Y_R, \quad \text{else } d = d_{\max}. \tag{6}$$

$$d' = \frac{\langle Y(t) - Y'_0 \rangle_+}{Y'_c}, \quad \text{if } d' < d_{\max},\ Y'(t) < Y'_S \text{ and } Y(t) < Y_R, \quad \text{else } d' = d_{\max}. \tag{7}$$

The meanings of the above used quantities are given in Tab. 1.

Table 1. Description of damage parameters

Y_C	$\left[(\text{Pa})^{1/2}\right]$	critical shear damage limit value
Y_0	$\left[(\text{Pa})^{1/2}\right]$	initial shear damage threshold value
Y'_C	$\left[(\text{Pa})^{1/2}\right]$	critical transverse damage limit value
Y'_0	$\left[(\text{Pa})^{1/2}\right]$	initial transverse damage threshold value
Y'_S	$\left[(\text{Pa})^{1/2}\right]$	brittle transverse damage limit of the fiber-matrix interface
Y_R	$\left[(\text{Pa})^{1/2}\right]$	elementary shear damage fracture limit
$d_{\max}$	[–]	maximum allowed value of d and d' ($d_{\max} < 1$)

Fiber tensile (compression) damage

The implemented law [3] implies that the fiber damage is null while $\varepsilon_{11} < \varepsilon_i^{ft}$, where ε_i^{ft} corresponds to the initial longitudinal fiber tensile damage threshold strain. Then the tensile fiber damage d^{ft} grows linearly between $\varepsilon_i^{ft} < \varepsilon_{11} < \varepsilon_u^{ft}$ where ε_u^{ft} is the ultimate longitudinal fiber tensile damage strain. When this ultimate value is reached, the fiber tensile damage d^{ft} reaches the ultimate damage, d_u^{ft}. After this point the tensile damage grows asymptotically towards $d^{ft} = 1$ (see Fig. 4).

5. PAM-Crash impact model validation

The PAM-Crash software includes many types of material models for composite materials as well as many element types. The Ladevèze model is chosen in this work for the analysis of impact behaviour together with shell elements. The properties of such model need to be firstly validated by experimental measurement for the chosen material. Therefore, a comparison of experimental measurement and numerical simulation in PAM-Crash is carried out. Investigated is transverse impact of metal impactor on composite plate (made of EHKF420-UD24K-40).

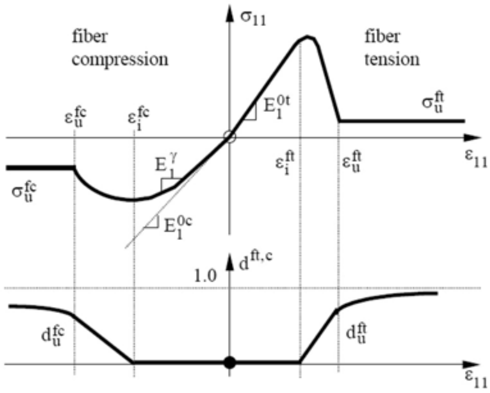

Fig. 4. Fibers tensile and compressive damage

Experimental measurements

A steel impactor was dropped from the height of $h = 300$ mm on a composite plate which was clamped along one edge was measured. A transverse displacement of the plate $u(t)$ was measured directly under the point of impact, 10 mm from the edge of the plate, see Fig. 5. The displacement was measured by a laser sensor optoNCDT by Micro-Epsilon. The experimental setup scheme is illustrated in Fig. 6.

The failure analysis of composite materials was the next comparison of the experimental measurement with numerical simulation [2]. Three stripes were made. The stripes properties were: length 105 mm, thickness 1.05 mm, width 15, 20, 25 mm and fiber orientation 0 (A00), 45 (A45) a 90 (A90). The comparison of experimental and numerical values of failure force are shown in Table. 4 bellow.

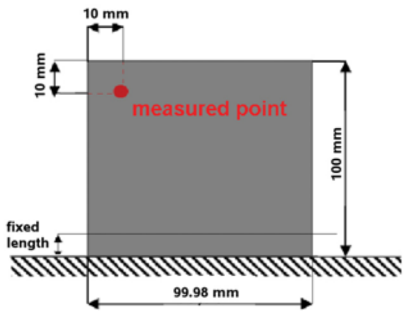

Fig. 5. Basic dimensions of composite plate

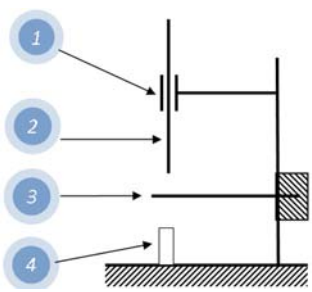

a)

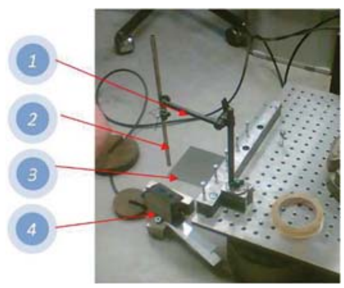

b)

Fig. 6. Experimental measurement: a) experimental schema, b) actual photograph from measurement (1 – tube fixture, 2 – impactor guide tube, 3 – composite plate, 4 – optoNCDT laser sensor)

Table 2. Plate properties

$E_L = 109.4$ GPa
$E_T = 7.7$ GPa
$G_{LT} = 4.5$ GPa
$\nu = 0.28$
fixed length = 6 mm
plate thickness = 0.8 mm
$\varrho = 1\,579.07$ kg/m^3

Table 3. Impactor properties

$E = 210$ GPa
$\varrho = 7\,800$ kg/m^3
$\nu = 0.3$
diameter $d = 4$ mm
length $l = 40$ mm

Table 4. Comparison of failure forces

Force [kN]	A00	A45	A90
Experiment	33.28	1.35	1.11
Numerical simulation	32.722 7	1.321 8	1.196 8

The composite plate made of carbon/epoxy (C/E) material consists of four layers of unidirectional composite with orientations $[0, 90, 90, 0]$. The total measured thickness is 0.84 mm. The dimensions of the plate including the measured point are given in Fig. 5. The characteristics of the plate are shown in Table 2, where the index L denotes the longitudinal direction and the index T means the transverse direction. The steel impactor is displayed in Fig. 7 and its basic material properties and dimensions are mentioned in Table 3. To eliminate errors seven measurements were carried out. The acquired time-dependent displacement curves are displayed in Fig. 8.

Fig. 7. Impactor

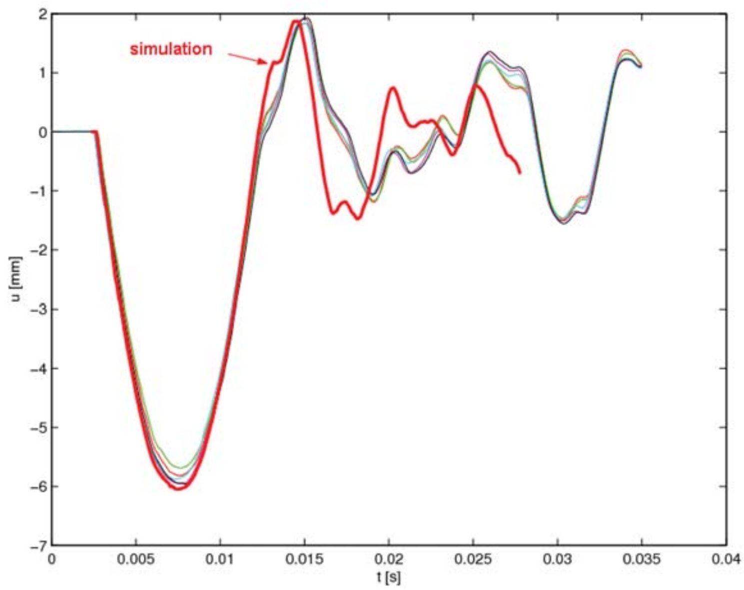

Fig. 8. Comparison between experimental curves and numerical simulation

Numerical simulations

The numerical model was firstly calibrated by means of modal analysis and calculation of free oscillations of the composite plate from an experimental measurement [1]. The following parameters are in Table 2. Material parameters of the steel impactor were chosen according to Table 3. The movement of the impactor was restricted by boundary conditions only to the direction normal to the plate. The resulting displacement curve obtained by numerical simulation is compared with the experimental curves in Fig. 8.

From the above-mentioned results it can be seen that there is a good agreement between experimental measurements and numerical simulation.

6. Design of new composite bumper reinforcement

In this part new composite bumper reinforcement is proposed. In the next step the stiffness analysis is performed. It is compared with an original steel bumper reinforcement by means of stiffness analysis. The aim was to keep the basic shape of the bumper reinforcement the same as in the case of the steel bumper – it means the length, height and curvature of bumper are similar. The goal is to achieve the same, eventually better, mechanical behaviour of the bumper reinforcement because the steel reinforcement shows fracture during RCAR test as discussed below. Afterwards, a large strain damage analysis and a weight comparison of selected bumper reinforcements are performed and the corresponding weights are compared. The connection between the reinforcement and the deformable element is not investigated. The connection is rigid and realized by so-called tied elements.

6.1. Stiffness analysis

For this stiffness analysis, four different simple geometry bumper reinforcement profiles were proposed as shown in Fig. 9.

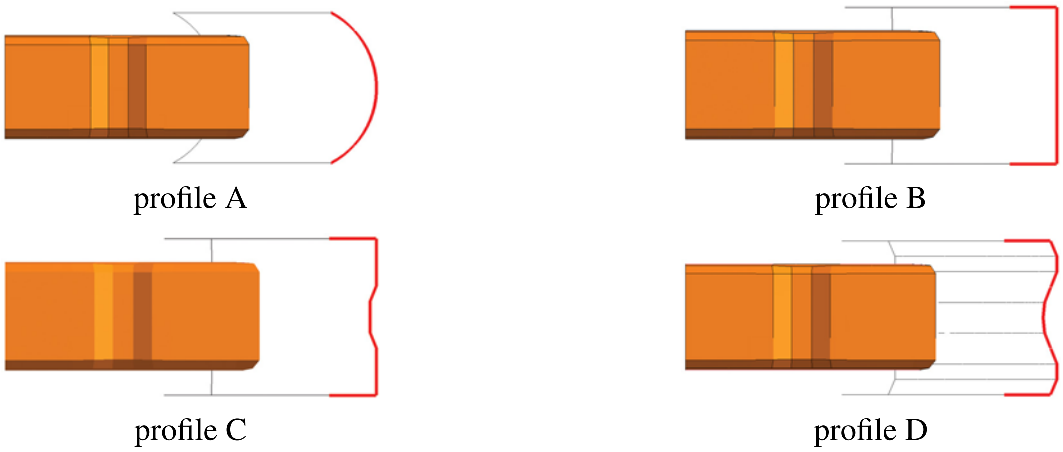

Fig. 9. Tested profiles (side view)

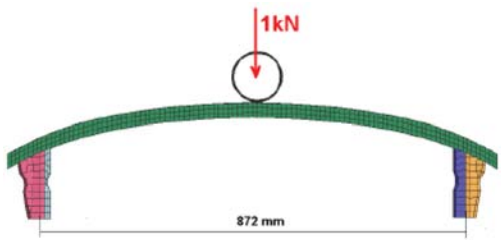

Fig. 10. Stiffness analysis

The stiffness test is displayed in Fig. 10. Steel cylindrical "impactor" is pushed into the bumper reinforcement with a force of 1 kN. The displacement of the bumper reinforcement is evaluated under the steel cylindrical position. The material used for bumper reinforcement is again EHKF420-UD24K-40 (C/E). Values of the Ladevèze model parameters were set as shown in Tab. 5.

Table 5. Values of Ladevèze model parameters.

Y_C	[(GPa)$^{1/2}$]	0.219
Y_0	[(GPa)$^{1/2}$]	0.219
Y_c'	[(GPa)$^{1/2}$]	0.204 9
Y_0'	[(GPa)$^{1/2}$]	0.204 9
Y_S'	[(GPa)$^{1/2}$]	0.011 700 42

Y_R	[(GPa)$^{1/2}$]	0.204 9
ε_i^{ft}	[–]	0.019 5
ε_u^{ft}	[–]	0.019 5
d_{max}	[–]	0.98

At first, the lay-up of the composite structure was proposed as [0[1], ± 30, 90, ∓ 30, 0] and the total composite thickness was 6 mm. This composite structure did not reach stiffness improvement in comparison with original steel bumper reinforcement (see [1]). The profiles A and C showed low stiffness values and, therefore, they were not taken into consideration in the next simulations. To further improve the designs, the composite structure lay-ups of both profiles B and D were modified to [0, ± 30, ∓ 30, 90, ± 30, ∓ 30, 0] in the next step and so the new total composite thickness was 7.6 mm. The new results are displayed in Fig. 11. It can be seen that the modified profiles are now stiffer than the original steel structure. The complete results from stiffness analysis can be found in [1].

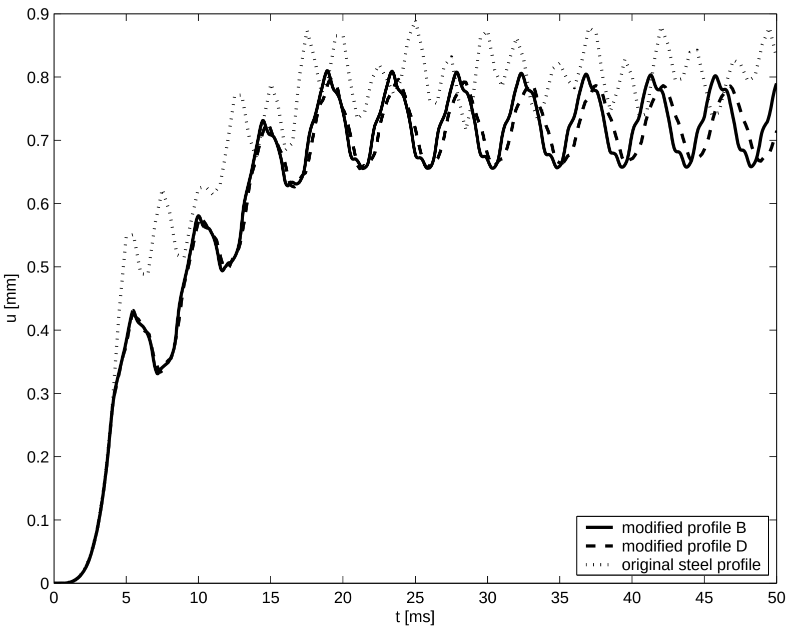

Fig. 11. Position of impactor in time

6.2. Damage analysis

The testing was realized with a rigid barrier, which was pushed against the bumper reinforcement and the deformable element, (see Fig. 12) by a prescribed displacement.

The parameters of the simulation barrier are equal to the barrier used in RCAR tests as introduced in section 2.2, i.e., rigid barrier with an inclination of 10 degrees, shift of the barrier is 40 % of the maximum width of the car without mirrors. The results are displayed in Fig. 13.

[1]bumper reinforcement longitudinal direction

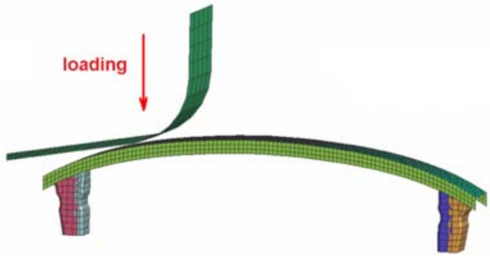

Fig. 12. Damage test

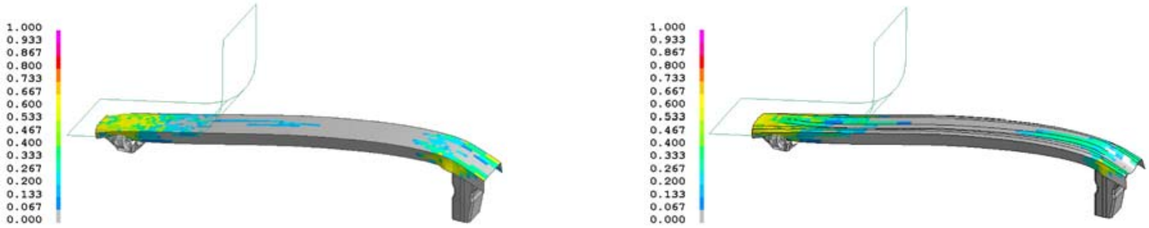

profile B profile D

Fig. 13. Damage of composite reinforcement in simulation time 20 ms

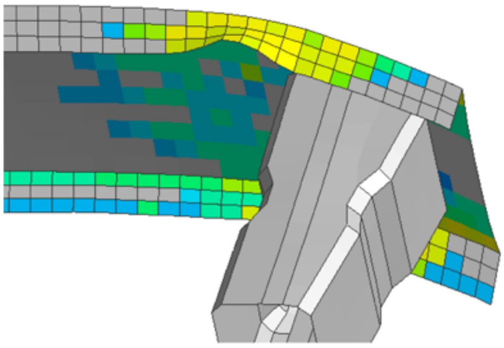

Fig. 14. The fracture initiation on the edge of modified profile B

The analysis revealed fracture on the edge of the profile B, see Fig. 14, which does not demonstrate a good damage behavior of the bumper reinforcement. The modified profile D proved to be the best of all tested profiles. The maximum value of damage in the simulation is about 60 % (maximum d_{max} value in the whole model). This means that the loading is still transferred to the deformable element (see Fig. 2) which is necessary feature for a well-designed bumper reinforcement. The original steel bumper reinforcement also shows certain fracture on the edge as shown in Fig. 15. Therefore, the composite profile D proved to be a suitable replacement for the original steel structure from both the stiffness and damage point of view.

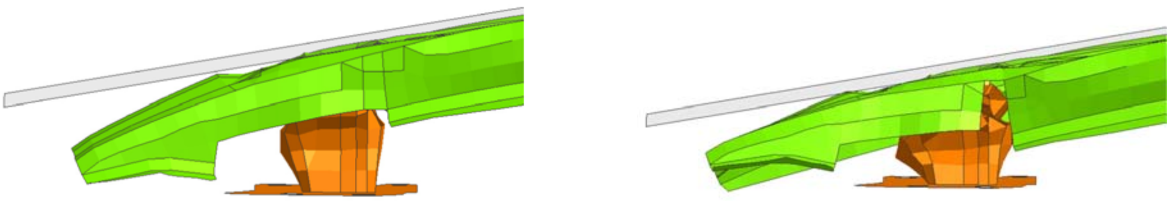

before fracture fracture

Fig. 15. Fracture on the original steel bumper reinforcement

The main advantage of the new bumper is the mass reduction. Mass comparison between original steel bumper reinforcement and composite bumper reinforcements is displayed in Tab. 6. The mass was calculated from elements volume and material density. The comparison shows a great mass reduction of the bumper reinforcements with use of the composite materials – up to 78 % in the case of best profile D.

Table 6. Bumper reinforcement mass comparison

Material	**Mass [kg]**
original steel	8.89
composite profile A	1.14
modified composite profile B	1.63
composite profile C	1.45
modified composite profile D	1.94

7. Conclusions

The work is dedicated to the simulation of car bumper behavior according to prescribed safety procedures. The main part of the work is focused on the design of a new composite bumper reinforcement with the aim to maintain or improve its mechanical properties while reducing the mass. The numerical models for PAM-Crash software using shell elements and Ledevèze model for the composite material are validated by experimental measurements. Afterward, four composite profiles are proposed and tested using stiffness analysis performed according to RCAR specification. After modification of the material structure, two profiles are found to have greater stiffness that the original steel structure and they are selected for latter damage analysis. The damage analysis proved one of the profile to be a suitable replacement for the original part as it showed no fracture and, moreover, a great mass reduction could be achieved with the use of the composite structure.

However, the matter of price and damage of the reinforcement due to composite material delamination must be further inspected. This problem has not been involved in the numerical model yet. The connection between the reinforcement and the deformable element was also not resolved in this work since it is rather a technological issue.

Acknowledgements

The work has been supported by the research project MSM 4977751303 and research project GA AV IAA200760611.

References

[1] Kleisner, V., Design of composite car bumper, Diploma thesis, University of West Bohemia, 2008. (in Czech)

[2] Laš, V., Zemčík, R., Progressive damage of unidirectional composite panels, Journal of Composite Materials, Vol. 42, No. 1, pp. 25–44, 2008.

[3] PAM-CRASH 2007. *Solver Notes Manual*. ESI-Group, Paris.

[4] Research Council for Automobile Repairs. *Rcar homepage* [on-line]. [cit. 2008-20-05]. URL: <http://www.rcar.org/index.htm>.

[5] The official site of the European New Car Assessment Programme. *Front impact* [on-line]. [cit. 2008-20-05]. URL: <http://www.euroncap.com/tests/frontimpact.aspx>.

[6] Vlk, F., Car body : ergonomics, biomechanics, passive safety, collision, structure, materials. Brno, Publisher Vlk, 2000, 243 pp., ISBN 80-238-5277-9. (in Czech)